

Isotropic Kink and Quasiparticle Excitations in the Three-Dimensional Perovskite Manganite $\text{La}_{0.6}\text{Sr}_{0.4}\text{MnO}_3$

Koji Horiba,^{1,*} Miho Kitamura,¹ Kohei Yoshimatsu,^{1,2} Makoto Minohara,¹ Enju Sakai,¹ Masaki Kobayashi,¹ Atsushi Fujimori,² and Hiroshi Kumigashira¹

¹*Photon Factory, Institute of Materials Structure Science, High Energy Accelerator Research Organization (KEK), 1-1 Oho, Tsukuba 305-0801, Japan*

²*Department of Physics, Graduate School of Science, The University of Tokyo, 7-3-1 Hongo, Bunkyo-ku, Tokyo 113-0033, Japan*

(Received 29 April 2015; published 17 February 2016)

In order to reveal the many-body interactions in three-dimensional perovskite manganites that show colossal magnetoresistance, we performed an *in situ* angle-resolved photoemission spectroscopy on $\text{La}_{0.6}\text{Sr}_{0.4}\text{MnO}_3$ and investigated the behavior of quasiparticles. We observed quasiparticle peaks near the Fermi momentum in both the electron and the hole bands, and clear kinks throughout the entire hole Fermi surface in the band dispersion. This isotropic behavior of quasiparticles and kinks suggests that polaronic quasiparticles produced by the coupling of electrons with Jahn-Teller phonons play an important role in the colossal magnetoresistance properties of the ferromagnetic metallic phase of three-dimensional manganites.

DOI: 10.1103/PhysRevLett.116.076401

$\text{La}_{1-x}\text{Sr}_x\text{MnO}_3$ is a typical hole-doped perovskite manganese oxide that has attracted considerable attention because of its unusual physical properties, such as “colossal” magnetoresistance (CMR) behavior and the half-metallic nature of its ground state; hence, it has potential for future spintronics applications [1]. These remarkable properties originate from the complex interplay between the charge, lattice, orbital, and spin degrees of freedom [2]. Consequently, the electronic and magnetic phases of $\text{La}_{1-x}\text{Sr}_x\text{MnO}_3$ are sensitive to changes in the strength of these mutual couplings, which results in rich phase diagrams for the manganites. In order to clarify the origin of these properties of $\text{La}_{1-x}\text{Sr}_x\text{MnO}_3$, understanding the detailed electronic band structures and interactions of electrons with various degrees of freedom and their anisotropic aspects is important. Angle-resolved photoemission spectroscopy (ARPES) is a powerful tool for investigating many-body interactions in quasiparticles as functions of binding energy and momentum [3]. From the line-shape analysis of the ARPES spectra, the momentum-resolved self-energy of quasiparticles, which reflects many-body interactions, has been widely examined in strongly correlated electron systems, most notably in the high- T_c cuprate superconductors [4,5].

For two-dimensional (2D) layered manganites, $N = 2$ in Ruddlesden-Popper phases with the chemical formula of $(\text{La}, \text{Sr})_{N+1}\text{Mn}_N\text{O}_{3N+1}$, the remnant Fermi-surface (FS) topology and the quasiparticle dynamics, which are coupled to collective excitations, have been investigated using ARPES measurements [6–11]. An ARPES study on bilayer manganites ($N = 2$) $\text{La}_{2-2x}\text{Sr}_{1+2x}\text{Mn}_2\text{O}_7$ with $x = 0.4$ revealed a pseudogap formation in the “antinodal” region and the existence of quasiparticle excitations in the nodal region; this leads to a nodal-antinodal dichotomous

characteristic similar to the characteristic feature of high- T_c cuprate superconductors [7]. In contrast, for the other compositions of the bilayer manganites with $x = 0.36$ – 0.38 , the existence of the quasiparticle peak even in the antinodal region and the isotropic behavior of kinks have been observed [8–10]. The composition dependence may be attributed to the increment of interlayer and/or intrabilayer coupling from $x = 0.4$ to $x = 0.36$. More recently, the disappearance of the pseudogap formation and isotropic interaction in the kink have also been reported in the intergrowth ($N > 2$) regions in bilayer manganites [11], which suggests the N dependence of mode coupling. However, despite intensive theoretical and experimental studies, the resultant relationship between the dimensionality N and the CMR properties, as well as whether kinks and quasiparticle excitations are isotropic or anisotropic as a function of N , remain controversial issues.

In order to provide a better understanding for the physics of manganites, it is indispensable to determine whether the kink observed in the layered manganites is inherent to 2D systems or also exists in three-dimensional (3D) perovskite manganite $\text{La}_{1-x}\text{Sr}_x\text{MnO}_3$, which corresponds to the $N = \infty$ limit of the Ruddlesden-Popper series. However, there does not seem to be any indication of the existence of the kink in $\text{La}_{1-x}\text{Sr}_x\text{MnO}_3$ even in the previously reported ARPES spectra near the Fermi level (E_F) [12–18]. This is partly because these previous studies mainly focused on valence band structures rather than low-energy excitations near E_F .

The lack of information concerning many-body interactions in the electronic structure near E_F in 3D manganites has hindered the understanding of the interaction between electrons and other degrees of freedom in the manganites. In particular, the absence of a kink in 3D manganites has

been questioned because relevant many-body interactions in strongly correlated oxides are also expected to be strong in 3D manganites. In this Letter, we report the observation of quasiparticle peaks and kinks in the band dispersion of 3D manganite $\text{La}_{0.6}\text{Sr}_{0.4}\text{MnO}_3$ (LSMO) through a precise and detailed investigation of the 3D electronic structure. *In situ* high energy-resolution ARPES measurements using the tunable excitation energy of synchrotron radiation enable us to trace the electronic structures in momentum space in every 3D direction. From their energy and momentum dependence, the interactions of electrons with other degrees of freedom are considered to be a possible origin of the kink in LSMO.

Samples of LSMO were grown on the atomically flat (001) surface of Nb-doped SrTiO_3 substrates by using a laser molecular beam epitaxy method. The growth conditions are detailed in Refs. [14] and [19]. The fabricated films were immediately transferred through an ultrahigh vacuum to the ARPES chamber without exposure to air [20]. The *in situ* ARPES measurements were carried out at beam line BL-28A and BL-2A MUSASHI of the Photon Factory (PF), KEK, at the sample temperature of 12 K using circular polarized synchrotron radiation as the excitation light source. The total energy and angular resolutions were set to approximately 20 meV and 0.3° , respectively. E_F of the samples was calibrated by measuring a gold foil that was electrically connected to the samples.

The LSMO films have a tetragonal crystal structure as a result of the epitaxial strain from the SrTiO_3 substrates [20–22]. In order to map the FS onto high-symmetry planes in the tetragonal Brillouin zone [Fig. 1(a)], photon energies of 88 eV for the $\Gamma X M$ plane and 60 eV for the $Z R A$ plane were selected, as shown in Fig. 1(b). Figures 1(c) and 1(d) display the results of the FS mapping at the photon energies of 88 and 60 eV, respectively. These results were obtained by plotting the intensity within the energy window of ± 20 meV from E_F in the ARPES spectra. Compared with the predicted FS from local-density-approximation calculations [14,23,24], we observed a small electron pocket centered around the Γ point and a large hole pocket centered around the A point. The dramatic changes in the FS with the photon energy and the good agreement between the ARPES results and local-density-approximation calculations indicate that our ARPES results do not reflect surface electronic structures but rather 3D bulk electronic structures with energy dispersion in the k_\perp direction. The finite density of states inside the electron and hole FSs centered around the Γ and A points, respectively, and the remnant FS in Fig. 1(c) centered around the M point, similar to the hole pocket around the A point in Fig. 1(d), are probably due to the effect of k_\perp broadening [15,16,25]. Very recently, an ARPES study using high-energy soft x rays (SX-ARPES), which has a large photoelectron escape depth and resultant better definition of momentum k_\perp , on a fractured single crystal of $\text{La}_{0.67}\text{Sr}_{0.33}\text{MnO}_3$ has been performed [18]. The overall FS topology derived from the SX-ARPES study was very similar

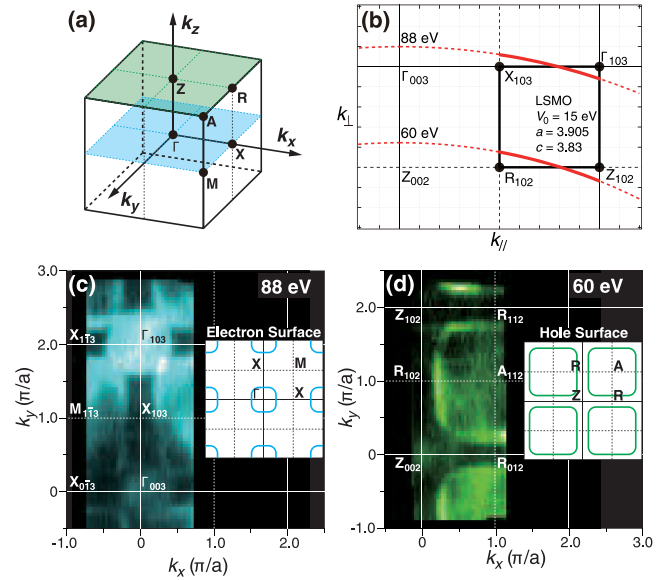


FIG. 1. (a) Brillouin zone for the tetragonal structure of epitaxially strained LSMO films. (b) Measured lines in momentum space for photon energies of 60 and 88 eV. (c) FS mapping for photon energies of 88 eV corresponding to the $\Gamma X M$ plane and (d) f 60 eV corresponding to the $Z R A$ plane. The insets in (c) and (d) illustrate the electron pocket around the Γ point and the hole pocket around the A point of the Brillouin zone, respectively, which were predicted by band structure calculations [14,24].

to that of the present results, which proves that our ARPES data largely reflect the bulk electronic structure of LSMO despite its surface sensitivity.

The energy dispersion of the bands that form the FS is shown in Fig. 2. For each FS, we observed a clear band dispersion with the Fermi cutoff, which reflects the metallic ground state of the LSMO. This is consistent with the results of the SX-ARPES study [18]. Pseudogap behavior due to a nesting instability observed in 2D manganites [6,7] was not observed in the ARPES spectra of the 3D LSMO. The energy distribution curves (EDCs) in Figs. 2(b) and 2(d) show small but distinct fine peak structures near E_F , which seem to have a “peak-dip-hump” structure, around the Fermi momentum (k_F) in both the electron and hole bands. In order to examine the possible coupling of quasiparticles with collective excitations, we analyzed the momentum distribution curves (MDCs) of the ARPES spectra. For the electron band, determining the exact MDC peak positions is difficult because of the substantial background due to the k_\perp broadening from the 3D small electron pocket [14–16]. Therefore, we concentrated on analyzing the hole band. Figure 3(a) shows an expanded plot of the intensity map in the near- E_F and near- k_F region for the hole band displayed in Fig. 2(c). The intensity modulation that is derived from the peak-dip-hump structure is also exhibited in the intensity plot of the hole band. Figure 3(b) displays the band dispersion obtained from the plot of the peak positions of the MDCs [26], which were determined by fitting the MDCs to the

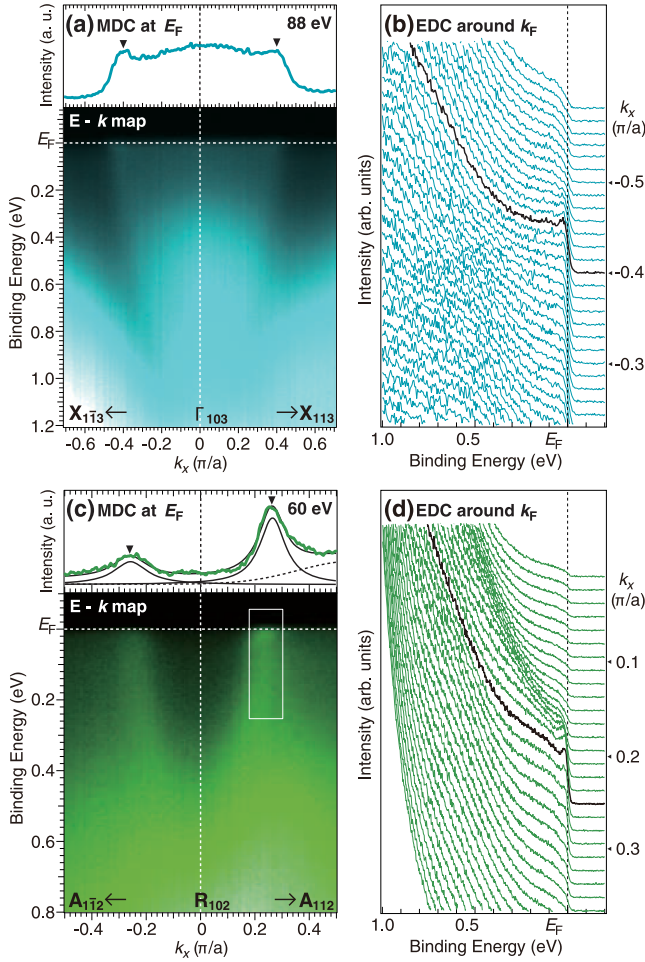


FIG. 2. ARPES spectra of LSMO films taken at photon energies of 88 eV along the Γ -X direction [(a) and (b)] and of 60 eV along the R-A direction [(c) and (d)]. (a) and (c) Intensity map of ARPES spectra (lower panels) and MDCs at E_F (upper panels). The filled triangles indicate the k_F points determined by the peaks in the MDCs. The MDC along the R-A direction were fitted to a linear combination of Lorentzians and a smooth background originating from the k_{\perp} broadening of the hole pocket, as seen in the upper panel of Fig. 2(c). A clear kink in the band dispersion was observed at the binding energy of approximately 50 meV, which corresponds well to the peak-dip-hump structures in the EDCs [27].

linear combination of Lorentzians and a smooth background originating from the k_{\perp} broadening of the hole pocket, as seen in the upper panel of Fig. 2(c). A clear kink in the band dispersion was observed at the binding energy of approximately 50 meV, which corresponds well to the peak-dip-hump structures in the EDCs [27].

From the observed kink, the effective mass enhancement factor was estimated from the ratio between the Fermi velocity v_F and the bare-band velocity v_b , as shown in Fig. 3(b). The obtained value of $m^*/m_b = v_b/v_F \sim 3$ suggests that the enhanced effective mass in LSMO may originate from a strong electron-boson coupling. In fact, this value is in good agreement with the effective mass which was deduced from the electronic specific heat coefficients [28], assuming that the interaction in the electron band is identical to that in the hole band. The

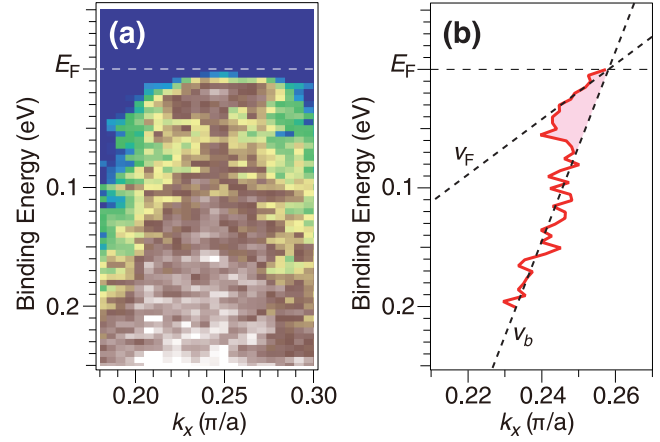


FIG. 3. (a) Expanded intensity map for the hole band in the near- E_F and near- k_F region [i.e., the box in Fig. 2(c)]. (b) Band dispersion along the R-A direction determined by tracing the peak positions of MDCs. The dashed lines are the results of fitting a line through k_F to band dispersions: One is for the band dispersion excluding the kink region to determine v_b , while the other is for the near- E_F region to determine v_F .

estimated coupling constant $\lambda = (m^*/m_b - 1) \sim 2$ in the electron-boson interaction in LSMO is comparable to the value of 1–4.6 in the 2D layered manganite $\text{La}_{2-2x}\text{Sr}_{1+2x}\text{Mn}_2\text{O}_7$ [7,8]. These values of λ in manganites are substantially larger than those in other strongly correlated perovskite oxides such as SrVO_3 [29] or Sr_2RuO_4 [30]. This indicates the existence of inherently strong electron-boson coupling in the 3D perovskite manganites as well as the 2D layered manganites.

The next crucial issue is whether or not the observed kink and quasiparticle peak show a momentum dependence. Figure 4 shows the ARPES results along different cuts in the hole FS. The isotropic nature of the kink and the quasiparticle peak was observed in the hole FS. Our ARPES results on the 3D LSMO provide evidence for the existence of the kink and the sharp quasiparticle peak along the $(0, \pi, \pi)$ to (π, π, π) directions (cut A), as shown in Figs. 3(b) and 2(d), respectively. Sharp edges at E_F and kinks were observed throughout the hole FS from cuts A to D in Fig. 4(a), although the quasiparticle intensity gradually decreased. Notably, the kinks have almost the same energies of around 50 meV and coupling constants of 1.5–2 [26] for all the band dispersions of the hole FS, as shown in Fig. 3(b) and Figs. 4(e)–4(g). Mannella *et al.* reported that the quasiparticle peak in $\text{La}_{2-2x}\text{Sr}_{1+2x}\text{Mn}_2\text{O}_7$ with $x = 0.4$ is sharpest along the $(0, 0)$ to (π, π) diagonal direction [7], which significantly differs from our results for the 3D LSMO. In contrast, finite quasiparticle intensities and isotropic kinks throughout the FS have been observed in $\text{La}_{2-2x}\text{Sr}_{1+2x}\text{Mn}_2\text{O}_7$ with $x = 0.36$ [10] and in the intergrowth $N > 2$ regions of $\text{La}_{2-2x}\text{Sr}_{1+2x}\text{Mn}_2\text{O}_7$ [11]; this is similar to our results for the 3D LSMO. In these previous reports on $\text{La}_{2-2x}\text{Sr}_{1+2x}\text{Mn}_2\text{O}_7$ [8–11], the reduced nesting instability resulting from the crossover from the 2D to 3D

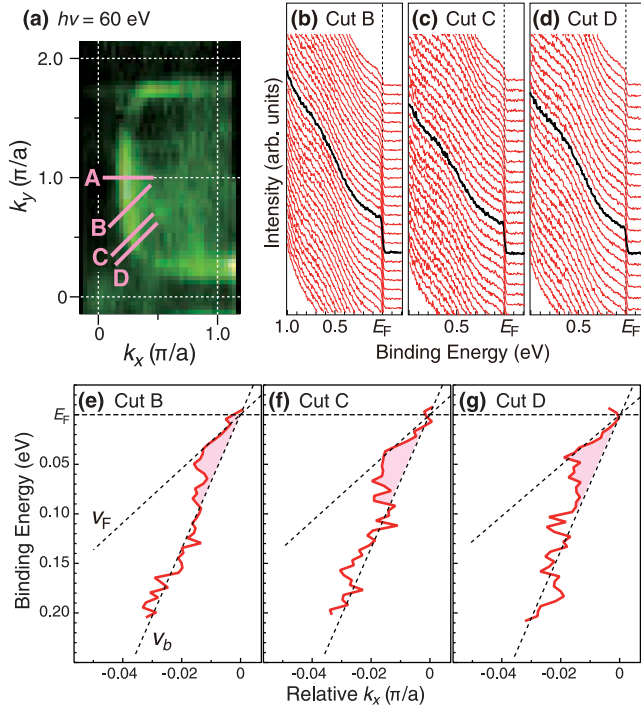


FIG. 4. (a) FS mapping for photon energy of 60 eV corresponding to the ZRA plane; this is a magnification of Fig. 1(d). (b)–(d) EDCs around k_F and (e)–(g) band dispersions obtained from the MDCs along cuts B–D, respectively, in (a). The black thick spectra in EDCs correspond to the spectra at the k_F points. Note that the EDCs around k_F and the band dispersion along a cut A are shown in Figs. 2(d) and Fig. 3(b), respectively. The dashed lines in (e)–(g) are the results of the linear fitting in the same way as Fig. 3(b).

ground states was considered to be the origin of the disappearance of the pseudogap behaviors that were reported by Mannella *et al.* [7]: The strength of the interlayer coupling increases with changing x from 0.4 in $\text{La}_{2-2x}\text{Sr}_{1+2x}\text{Mn}_2\text{O}_7$ [8–10], while N becomes more than 2 in the stacking-fault intergrowth region of $\text{La}_{2-2x}\text{Sr}_{1+2x}\text{Mn}_2\text{O}_7$ [11]. Since the 3D LSMO is regarded as the $N = \infty$ limit of layered manganites, its nesting instability is expected to be considerably weakened because of the strong “interlayer coupling.” Therefore, the finite quasiparticle intensities and isotropic kinks throughout the FS are suggested to be common phenomena of both the 2D and 3D manganites without the nesting instability.

Strongly localized bosons coupled with electrons most likely cause these isotropic kinks in the momentum space of 3D manganites. We consider two plausible interactions in order to clarify the origin of the quasiparticle excitation and resulting kinks in LSMO, the coupling of electrons with magnetic excitations and the coupling of electrons with phonon modes. Concerning the coupling of electrons with the magnetic excitations (i.e., ferromagnetic magnons in double-exchange manganites), spin wave dispersions throughout the Brillouin zone have been investigated by using the inelastic neutron scattering on $\text{La}_{0.7}\text{Pb}_{0.3}\text{MnO}_3$ [31]. The magnon band is highly dispersive and has a bandwidth of ~ 100 meV.

This suggests that electron-magnon interactions are broadened in the energy scale and limited to particular regions in momentum space, which are defined with critical momentum transfer vectors. Consequently, we expect the quasiparticle excitation and kink to have a large anisotropy in momentum space. Moreover, the half-metallic electronic structure of LSMO does not allow magnon excitations to scatter electrons near E_F because spin-flip scattering cannot occur near E_F owing to the full spin polarization.

For the coupling with phonon modes, phonon dispersions have also been determined by using inelastic neutron scattering on $\text{La}_{0.7}\text{Sr}_{0.3}\text{MnO}_3$ [32,33]. Several less-dispersive, namely relatively localized phonon branches were observed around the energy of 50 meV. In particular, phonon branches derived from the excitation of Jahn-Teller (JT) phonon modes with bending, linear breathing, and stretching characters are located at the energies of ~ 37 meV, ~ 45 meV, and ~ 71 meV at the Γ point, respectively. These are close to the kink energy observed in the ARPES band dispersions. Therefore, it is reasonable to conclude that the kink in the band dispersions results from the interaction of electrons with JT phonon modes. Note that such a series of JT phonon modes in this energy region has been also observed by optical conductivity measurements of $\text{La}_{1-x}\text{Sr}_x\text{MnO}_3$ polycrystalline samples [34] and thin films [35,36], as well as in 2D manganites [37]. Strong interaction between electrons and local JT phonons in LSMO has been considered to lead to the formation of JT small polarons. However, the observation of well-defined quasiparticles at least near E_F indicates that electrons (or holes) around E_F basically form energy bands and that the polaronic interaction is not stronger than that expected from the ideal small polaron picture in the present 3D manganites [18]. JT distortions are collectively excited by electron (or hole) hopping between JT active Mn^{3+} and inactive Mn^{4+} ions. Consequently, the effective mass of quasiparticles is enhanced, even in the ferromagnetic metallic phase in LSMO. Indeed, a polaronic signature in ferromagnetic metallic manganites was recently observed in a scanning tunneling spectroscopic study on $\text{La}_{0.7}\text{Ca}_{0.3}\text{MnO}_3$ [38].

In summary, we have performed an *in situ* ARPES study on 3D LSMO and found isotropic quasiparticle excitation peaks and kinks in the experimental band dispersions. The observed isotropic and strong renormalization of the band dispersions suggests that the electrons strongly interact with local JT phonons and that the polaronic quasiparticles play an important role in the CMR behavior of the ferromagnetic metallic phase of LSMO. Our findings will contribute to understanding the universal physics among 2D and 3D manganites with regard to the origin of CMR phenomena.

The authors are very grateful to Professor T. Yoshida and Professor K. Ishizaka for fruitful discussions. This work was supported by a Grant-in-Aid for Scientific Research (No. B25287095 and No. S22224005) and a Grant-in-Aid for Young Scientists (No. 26870843) from the Japan Society for the Promotion of Science (JSPS) as well as

the MEXT Elements Strategy Initiative to Form Core Research Center. M.K. acknowledges financial support from JSPS for Young Scientists. This work at KEK-PF was performed under the approval of the Program Advisory Committee (Proposals No. 2012G536, No. 2012G688, No. 2013S2-002, and No. 2015S2-005) at the Institute of Materials Structure Science, KEK.

*horiba@post.kek.jp

- [1] *Colossal Magnetoresistive Oxides*, edited by Y. Tokura, Advances in Condensed Matter Science Vol. 2 (Gordon and Breach, Amsterdam, 2000).
- [2] M. Imada, A. Fujimori, and Y. Tokura, *Rev. Mod. Phys.* **70**, 1039 (1998).
- [3] S. Hüfner, *Very High Resolution Photoelectron Spectroscopy* (Springer, New York, 2007).
- [4] T. Valla, A. V. Fedorov, P. D. Johnson, B. O. Wells, S. L. Hulbert, Q. Li, G. D. Gu, and N. Koshizuka, *Science* **285**, 2110 (1999).
- [5] A. Damascelli, Z. Hussain, and Z.-X. Shen, *Rev. Mod. Phys.* **75**, 473 (2003).
- [6] Y.-D. Chuang, A. D. Gromko, D. S. Dessau, T. Kimura, and Y. Tokura, *Science* **292**, 1509 (2001).
- [7] N. Mannella, W. L. Yang, X. J. Zhou, H. Zheng, J. F. Mitchell, J. Zaanen, T. P. Devereaux, N. Nagaosa, Z. Hussain, and Z.-X. Shen, *Nature (London)* **438**, 474 (2005).
- [8] Z. Sun, Y.-D. Chuang, A. V. Fedorov, J. F. Douglas, D. Reznik, F. Weber, N. Aliouane, D. N. Argyriou, H. Zheng, J. F. Mitchell, T. Kimura, Y. Tokura, A. Revcolevschi, and D. S. Dessau, *Phys. Rev. Lett.* **97**, 056401 (2006).
- [9] Z. Sun, J. F. Douglas, A. V. Fedorov, Y.-D. Chuang, H. Zheng, J. F. Mitchell, and D. S. Dessau, *Nat. Phys.* **3**, 248 (2007).
- [10] S. de Jong, Y. Huang, I. Santoso, F. Massee, R. Follath, O. Schwarzkopf, L. Patthey, M. Shi, and M. S. Golden, *Phys. Rev. B* **76**, 235117 (2007).
- [11] F. Massee, S. de Jong, Y. Huang, W. K. Siu, I. Santoso, A. Mans, A. T. Boothroyd, D. Prabhakaran, R. Follath, A. Varykhalov, L. Patthey, M. Shi, J. B. Goedkoop, and M. S. Golden, *Nat. Phys.* **7**, 978 (2011).
- [12] M. Shi, M. C. Falub, P. R. Willmott, J. Krempasky, R. Herger, K. Hricovini, and L. Patthey, *Phys. Rev. B* **70**, 140407(R) (2004).
- [13] M. C. Falub, M. Shi, P. R. Willmott, J. Krempasky, S. G. Chiuzbaian, K. Hricovini, and L. Patthey, *Phys. Rev. B* **72**, 054444 (2005).
- [14] A. Chikamatsu, H. Wadati, H. Kumigashira, M. Oshima, A. Fujimori, N. Hamada, T. Ohnishi, M. Lippmaa, K. Ono, M. Kawasaki, and H. Koinuma, *Phys. Rev. B* **73**, 195105 (2006).
- [15] J. Krempaský, V. N. Strocov, L. Patthey, P. R. Willmott, R. Herger, M. Falub, P. Blaha, M. Hoesch, V. Petrov, M. C. Richter, O. Heckmann, and K. Hricovini, *Phys. Rev. B* **77**, 165120 (2008).
- [16] J. Krempaský, V. N. Strocov, P. Blaha, L. Patthey, M. Radović, M. Falub, M. Shi, and K. Hricovini, *J. Electron Spectrosc. Relat. Phenom.* **181**, 63 (2010).
- [17] A. Tebano, A. Orsini, P. G. Medaglia, D. Di Castro, G. Balestrino, B. Freelon, A. Bostwick, Y. J. Chang, G. Gaines, E. Rotenberg, and N. L. Saini, *Phys. Rev. B* **82**, 214407 (2010).
- [18] L. L. Lev, J. Krempaský, U. Staub, V. A. Rogalev, T. Schmitt, M. Shi, P. Blaha, A. S. Mishchenko, A. A. Veligzhanin, Y. V. Zubavichus, M. B. Tsetlin, H. Volfová, J. Braun, J. Minár, and V. N. Strocov, *Phys. Rev. Lett.* **114**, 237601 (2015).
- [19] K. Horiba, A. Chikamatsu, H. Kumigashira, M. Oshima, N. Nakagawa, M. Lippmaa, K. Ono, M. Kawasaki, and H. Koinuma, *Phys. Rev. B* **71**, 155420 (2005).
- [20] K. Horiba, H. Ohguchi, H. Kumigashira, M. Oshima, K. Ono, N. Nakagawa, M. Lippmaa, M. Kawasaki, and H. Koinuma, *Rev. Sci. Instrum.* **74**, 3406 (2003).
- [21] M. Izumi, Y. Konishi, T. Nishihara, S. Hayashi, M. Shinohara, M. Kawasaki, and Y. Tokura, *Appl. Phys. Lett.* **73**, 2497 (1998).
- [22] Y. Konishi, Z. Fang, M. Izumi, T. Manako, M. Kasai, H. Kuwahara, M. Kawasaki, K. Terakura, and Y. Tokura, *J. Phys. Soc. Jpn.* **68**, 3790 (1999).
- [23] N. Hamada *et al.* (unpublished).
- [24] E. A. Livesay, R. N. West, S. B. Dugdale, G. Santi, and T. Jarlborg, *J. Phys. Condens. Matter* **11**, L279 (1999).
- [25] H. Wadati, T. Yoshida, A. Chikamatsu, H. Kumigashira, M. Oshima, H. Eisaki, Z.-X. Shen, T. Mizokawa, and A. Fujimori, *Phase Transitions* **79**, 617 (2006).
- [26] See Supplemental Material at <http://link.aps.org/supplemental/10.1103/PhysRevLett.116.076401>, which includes Refs. [20–22], for more details about the analytical procedure for MDC, the band dispersion in the high-energy region, characterization of the epitaxial strain of LSMO films, and kink along the nodal direction and isotropy of the coupling constant.
- [27] We do not find any signature of a “high-energy kink” [J. Graf *et al.*, *Phys. Rev. Lett.* **98**, 067004 (2007)] in the high-energy region of the band dispersion [26].
- [28] T. Okuda, A. Asamitsu, Y. Tomioka, T. Kimura, Y. Taguchi, and Y. Tokura, *Phys. Rev. Lett.* **81**, 3203 (1998).
- [29] S. Aizaki, T. Yoshida, K. Yoshimatsu, M. Takizawa, M. Minohara, S. Ideta, A. Fujimori, K. Gupta, P. Mahadevan, K. Horiba, H. Kumigashira, and M. Oshima, *Phys. Rev. Lett.* **109**, 056401 (2012).
- [30] Y. Aiura, Y. Yoshida, I. Hase, S. I. Ikeda, M. Higashiguchi, X. Y. Cui, K. Shimada, H. Namatame, M. Taniguchi, and H. Bando, *Phys. Rev. Lett.* **93**, 117005 (2004).
- [31] T. G. Perring, G. Aeppli, S. M. Hayden, S. A. Carter, J. P. Remeika, and S.-W. Cheong, *Phys. Rev. Lett.* **77**, 711 (1996).
- [32] W. Reichardt and M. Braden, *Physica (Amsterdam)* **263B–264B**, 416 (1999).
- [33] J. Zhang, P. Dai, J. A. Fernandez-Baca, E. W. Plummer, Y. Tomioka, and Y. Tokura, *Phys. Rev. Lett.* **86**, 3823 (2001).
- [34] J. H. Jung, K. H. Kim, H. J. Lee, J. S. Ahn, N. J. Hur, T. W. Noh, M. S. Kim, and J.-G. Park, *Phys. Rev. B* **59**, 3793 (1999).
- [35] Ch. Hartinger, F. Mayr, A. Loidl, and T. Kopp, *Phys. Rev. B* **70**, 134415 (2004).
- [36] A. M. Haghiri-Gosnet, M. Koubaa, A. F. Santander-Syro, R. P. S. M. Lobo, Ph. Lecoeur, and B. Mercey, *Phys. Rev. B* **78**, 115118 (2008).
- [37] H. M. Rønnow, Ch. Renner, G. Aeppli, T. Kimura, and Y. Tokura, *Nature (London)* **440**, 1025 (2006).
- [38] S. Seiro, Y. Fasano, I. Maggio-Aprile, E. Koller, O. Kuffer, and Ø. Fischer, *Phys. Rev. B* **77**, 020407(R) (2008).